PAPER

Design, Modeling and Optimization of an Ocean Wave Power Generation Buoy

AUTHORS

Carlos Velez
Department of Mechanical and Aerospace Engineering, University of Central Florida

Zhihua Qu
Department of Electrical Engineering and Computer Science, University of Central Florida

Kuo-Chi Lin
Department of Mechanical and Aerospace Engineering, University of Central Florida

Shiyuan Jin
Department of Electrical Engineering and Computer Science, University of Central Florida

ABSTRACT

Ocean waves provide an abundant, clean, and renewable source of energy. Existing systems, typically hydraulic turbines powered by high-pressure fluids, are very large in size and costly. Additionally, they require large ocean waves in which to operate. This paper details the design, development, and laboratory prototype testing of a wave power generation system comprising a buoy that houses a set of mechanical devices and a permanent magnetic generator. The buoy, floating on the surface of the ocean, utilizes the vertical movement of ocean waves to pull on a chain anchored to the ocean floor. The linear motion is translated into rotation, which rotates a shaft to move armature coils within the generator to produce an electric current. The amount of energy generated increases with wave height and input frequency. The flywheel inertia, shaft rotation speed, and electrical load are optimized to provide maximize electricity production. The paper addresses the design, analysis, and implementation of mechanical and electrical systems, together with resistive load control, system optimization, and performance analysis. Both simulation and experimental results are provided and compared.

Keywords: buoy, ocean wave energy, permanent magnetic generator, load control, wave power generation

Introduction

Research into safe and clean energy harvesting from renewable sources has become popular in response to the current energy crisis and growing environmental awareness. Renewable energy sources principally include solar, wind, hydroelectric, ocean waves, etc. Wind and solar power are restricted to specific geographic regions; wind power is only useful in windy areas, and solar power is effective in only sunny ones. Ocean wave power is especially promising because more than two thirds of the Earth's surface is covered by ocean, which should allow wise access across the globe. Nature offers large amounts of kinetic energy in the form of ocean waves, and it is estimated that if 0.2% of the untapped energy of the ocean could be harvested, it could provide power sufficient for the entire world (Falnes, 2002).

This paper presents the novel design, development, and laboratory prototype testing of the wave power generation system, shown in Figure 1, in which a set of mechanical devices and a permanent magnetic generator are installed inside a buoy. The buoy floats on the surface of the ocean and utilizes the vertical movement of ocean waves to generate electric power. Specifically, when the buoy moves from the trough to the crest, the buoyancy force and hydrodynamic force pull upon the chain anchored to the ocean floor and rotates the shaft to move armature coils of the generator to produce electricity; meanwhile, the coiled spring in the reel is pulled and tightened. Similarly, when the buoy moves from the crest to the trough, the reel rewinds the cable, and the system returns to its original state.

The project thus far can be broken into three stages:

1. Before implementing the laboratory prototype, a Matlab simulation was used to simulate the hydrodynamics and the mechanical and electrical models. The simulation process aided the optimization of the system's electric power output.
2. Next, the laboratory prototype was constructed and selected data were measured.
3. Finally, the prototype results were analyzed. Laboratory prototype data were compared with simulation data and identified discrepancies were analyzed.

This design incorporates many technically challenging components such

FIGURE 1

Conceptual design, wave power generation.

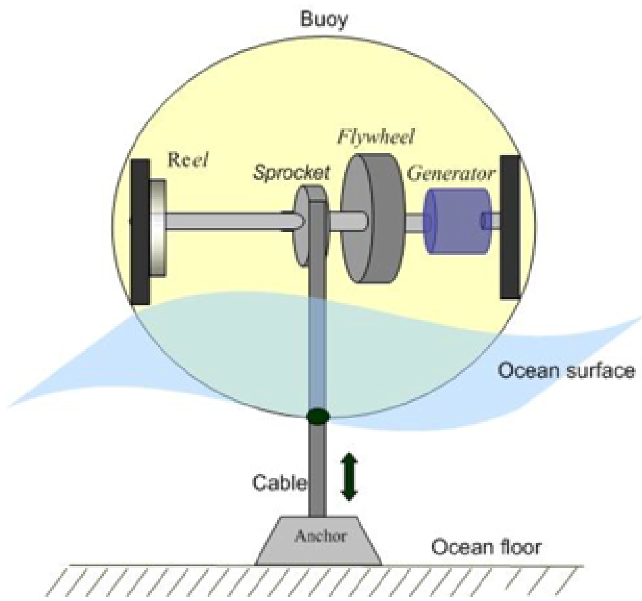

as the wet-dry interface of the cable, mooring design, hazardous environmental effects such as biofouling, and multidirectional buoy motion. These components are needed for field installation but are not currently considered as they are outside the scope of this theoretical mechanical study. The objective of this paper is to study and optimize solely the internal mechanical components within the buoy for a one-dimensional oscillating wave motion. System optimization was done by integrating the hydrodynamic model along with the mechanical and electric models. Additionally, load control was applied to vary the electrical load on the output of the generator and to regulate the rotor rpm in the case of irregular wave motion.

The remainder of the paper is organized as follows:

- Existing Wave Power Generation Technologies introduces existing ocean wave power generation technologies.
- Laboratory Prototype Design introduces conceptual and laboratory prototype designs.
- Mathematical Model provides the mathematical equations and theoretical analysis.
- System Optimization addresses system optimization (including simulation and prototyping test results).
- Results and Discussion provides experimental results and discussion of voltage output, tension measurement, RPM, and electrical power output.
- Conclusion concludes the paper.

Existing Wave Power Generation Technologies

Compared with other forms of generation of electricity such as wind and hydro power, research on wave energy is still in its infancy. Wave energy development is a field that requires multidisciplined, cooperative efforts including technologies in hydrodynamics, mechanical engineering, in addition to control and power systems. There is much to improve in system efficiency, cost, reliability, and scalability to make the extraction of wave energy practical for consumer use. A few typical wave energy development examples are listed below.

- Conceptual Wave Park by Oregon State University (Brekken et al., 2009): OSU is the pioneer in research and development of wave energy in the United States. It is reported that a network of about 500 buoys could power the business district of downtown Portland. Its linear generator using linear translational motion harvests energy from one directional motion of a buoy.
- JAMSTEC, Japan (Osawa et al., 2002): This system contains three air chambers that convert wave energy into pneumatic energy. Wave action causes the internal water level in each chamber to rise and fall, forcing a bidirectional airflow over an air turbine. The turbines drive three induction generators to produce a three-phase AC output at 200 Volts. More research has been done by Cunha et al. (2009), Elwood et al. (2010), Haniotis et al. (2002), Kimoulakis et al. (2008), Leijon et al. (2005), Mueller and Baker (2002), Rhinefrank et al. (2006), and Wolfbrandt (2006).

These systems all share the same difficulty in converting the oscillatory motion of waves to the rotation of a permanent magnet generator. The proposed concept utilizes a buoy to convert its linear height displacement into electrical energy. The vertical displacement of the buoy will enable a chain to rotate the shaft of a generator installed within the buoy itself. Through the use of a pulley system, the rotation of the generator shaft will be amplified with respect to the actual buoy displacement. Incorporating these components will lead to a small, inexpensive, light-weight and consistent form of producing energy for the applications including the powering of nearby coastal regions or offshore platforms.

Laboratory Prototype Design

The prototype mechanical system has been designed and constructed and can convert the kinetic energy developed from the heaving forces generated by ocean waves into electrical energy. The internal mechanism of the buoy is designed to translate the vertical oscillations of a buoy into rotational energy that will power a generator. Figure 2 is a snapshot of wave power generation system inside the buoy.

Mechanical Components

In Figure 2, a single long chain wraps around two sets of sprockets on the rotor shaft (connected to the generator) and then loops downward and is wrapped around two rotational bearings fixed to the laboratory floor. There are two loops made by a single chain connecting the moving rotor with the fixed rotor. This double loop design multiplies the chain velocity at the second loop/sprocket by a factor of 4. Additionally, the double loop design allows for unidirectional rotation of the main rotor (shown in Figure 2) independent of the direction of motion of the chain/buoy. In effect, even if the buoy is oscillating up and down, it will only incur a clockwise directional torque on the generator shaft. In order for the chain to loop around and drive the rotor shaft, two sprockets are required. The first sprocket is located at the first chain loop where clockwise rotation will drive the rotor; during counter-clockwise rotation, it will spin freely around the main rotor. The second sprocket is located where the chain loops around the rotor for the second time. This sprocket is reversed and operates opposite to the first sprocket. When the buoy moves upward, the first sprocket drives the generator and the second sprocket spins freely. The opposite is true for the downward motion of the buoy, resulting in unidirectional rotation of the rotor with bidirectional motion of the buoy/chain. One end of the chain is attached to a constant torque rotational spring, which acts to keep tension in the chain, and the other end of the chain is fixed to the moving buoy. This rotational spring also helps drive the shaft in order to ensure the continued rotation of the shaft. The shaft is coupled to a permanent magnet generator, which extracts power from the rotating motion of the shaft. To increase the inertia of the shaft assembly, three steel flywheels are fastened onto the driven shaft.

In order to test the performance of the mechanical system, a 6-DOF motion table is utilized to simulate the motion of a wave. The motion of the platform is prescribed to follow a sinusoidal path in the vertical direction only. The mechanism is placed on top of the platform with the chain fixed to the floor, simulating a mooring to the ocean floor. The platform was programmed to move at various frequencies ranging from 0.1 to 0.3 Hertz and at amplitudes of 5–15 cm.

FIGURE 2

Prototype wave generation system.

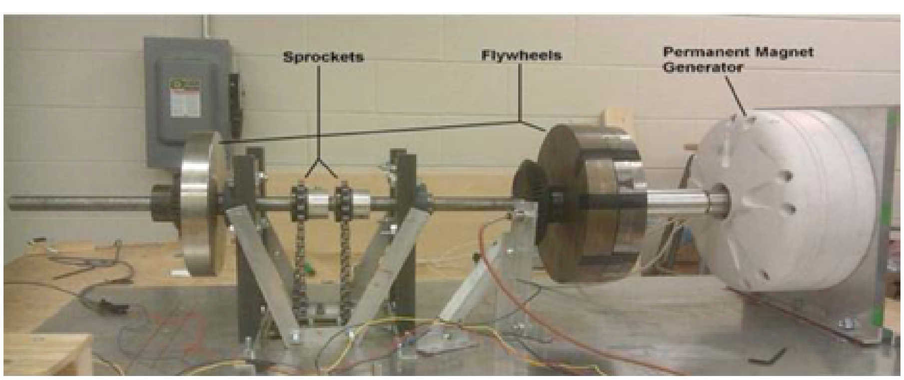

Electrical Components

In order to analyze the performance of the mechanism, several parameters were measured during the experiments.

- An optical sensor was used to measure the instantaneous RPM of the shaft.
- A potentiometer was used to measure the instantaneous location of the platform.
- A strain gauge was placed on one of the links in the chain in order to constantly measure tension in the chain.
- A Data Acquisition Board (DAQ) measured the power output from the generator; the three leads of the generator are brought out and connected to a diode rectifier.

A program constructed in LABVIEW controlled a relay switch.

The relay switch position is dependent on the shaft RPM and position of the platform. When load is applied, the load current flows inside the generator, inducing a voltage drop across the internal circuit resistance. Applying additional resistance increases the torque of the generator, thereby reducing the RPM.

Design Issues Regarding Optimal Performance

Components within the mechanical system can be optimized to improve overall system performance. The optimal performance is intended to produce the largest amount of power, while preventing the system from experiencing any large peak or cyclical stresses that would greatly limit the life span of the mechanism.

The amount of inertia contributed by the flywheels is one simple way to optimize the efficiency of the system. By increasing the inertia of the shaft, one raises the potential energy in the rotating shaft. Consequently, the torque needed to rotate the shaft at a set RPM is increased because of the increase in inertia. The proper amount of shaft inertia is determined by the size of the ocean waves, and this will subsequently drive the dimensions of the buoy. Additionally a gear train may be implemented to convert excess torque into an increased RPM of the shaft; increasing the gear ratio will proportionally increase the shaft speed. Thus, the gear ratio should be optimized to increase the RPM of the shaft while not limiting the motion of the buoy too much through the increase in mass. The dimensions of the sprockets can also be optimized to improve the performance of the overall system. Reducing the radius of the sprocket increases the shaft RPM and reduces the amount of torque created by the buoy. The method in which the generator extracts energy from the rotating shaft can be selected to conserve the momentum of the flywheels. Varying the electrical resistance or load on the generator can allow one to control the required torque needed to drive the generator. A detailed analytical solution is developed to optimize the system components and is addressed at the optimization section of this paper.

Mathematical Model

Laboratory Prototype Model

The system can be represented by three models: hydrodynamic model, generator motion model, and buoy model, as illustrated in Figure 3.

The relationship between mechanical and electrical torques and angular acceleration can be represented by the following equation:

$$T_m - T_e = I\frac{d\omega}{dt} \quad (1)$$

where T_m is the mechanical torque, T_e is the electromagnetic back-torque, I is the moment of inertia of the system, and ω is the angular velocity of the shaft. The mechanical torque is created by both the tension from the tethered cable as well as system frictional force. The electrical torque is developed by the rotor of the generator as it rotates in the magnetic field with a resistive load applied to the generator.

FIGURE 3

Hydrodynamic and buoy system model.

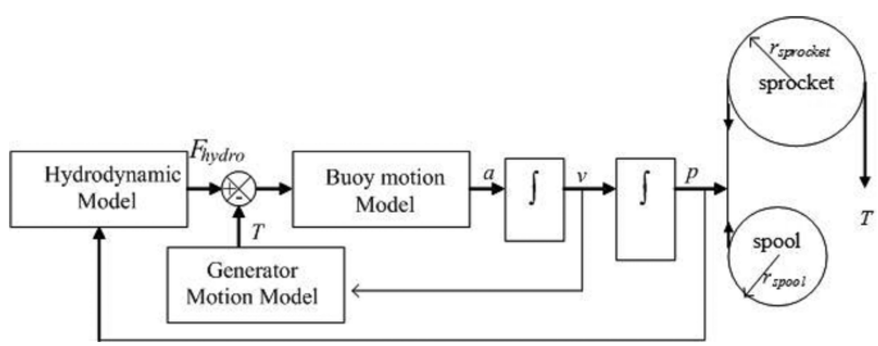

Hydrodynamic Model

The ocean wave motion is transferred into rotational motion for the permanent magnetic generator via the motion imparted on the floating buoy. Wave forces consist of both rotational and heaving forces. In this paper, only the one-dimensional heaving force is considered in the hydrodynamic model. The equation of motion is modeled by the following:

$$m\ddot{z} = F_b + F_{excite} - F_{drag} - mg - T \quad (2)$$

where m is the total mass of the buoy including all components inside it, z is the vertical displacement of the buoy, F_B is the buoyance force acting on the buoy, F_{excite} is the vertical wave excitation force which is described shortly, F_{drag} is the hydrodynamic drag force acting on the buoy, and T is the tension force of the cable which tethers the buoy to ocean floor (Sarpkaya & Isaacson, 1981). F_B, F_{drag}, T, and F_{excite} can be calculated as follows.

$$F_b = \rho_w g V_{submerged} \quad (3)$$

where w is the water density and $V_{submerged}$ is the submerged volume of the buoy. When a spherical buoy is in hydrostatic equilibrium, the weight of the buoy is balanced by the buoyancy force. Assuming that the water level reaches a height of y0 above the center of the sphere, then the overall static buoyancy force experienced by the buoy is governed by the following equation

$$F_b = \rho_w g \left[\frac{2}{3}\pi R^3 + \pi\left(R^2 y_o - \frac{1}{3}y_o^3\right)\right] \tag{4}$$

where ρ_w is the density of the water (displaced fluid) and R is the radius of the spherical buoy.

Next, the drag force (F_D) in equation (2) is expressed analytically as

$$F_{drag} = -\frac{1}{2}\rho_w C_d A_b |\dot{z}||\dot{z}| \tag{5}$$

where C_d, set to 0.75, is the drag coefficient of the buoy and A_b is the area of the submerged surface of the buoy projected on a plane normal to the z-direction. The drag coefficient, C_d, is a function of the geometry of the buoy and the Reynolds number of the fluid, but for convenience purposes it will be modeled as a constant for this paper (Leonard et al., 2000). The drag force contributes the least of the five forces due to its low velocity ($\dot{z}$).

The cable tension force (T) in equation (2) is expressed as

$$T = T_o + D_{coupled} * \left(C_{load} * \frac{C_{gen}\omega}{r} + \frac{I\alpha}{r}\right)$$

$$C_{load} = \begin{cases} 1 & \text{if load is on} \\ 0 & \text{if otherwise} \end{cases}$$

$$D_{coupled} = \begin{cases} 1 & \text{Coupled} \\ 0 & \text{Uncoupled} \end{cases} \tag{6, 7, 8}$$

where C_{load} represents the electrical load state, C_{gen} is the generator back-torque coefficient (generation load), $D_{coupled}$ represents the coupled/uncoupled state of the mechanical system discussed shortly, α is the angular acceleration of the shaft, and r is the radius of the sprocket.

The last force in equation (2) is the wave excitation force. The excitation force of a wave acting on a body can be separated into three components: the Froude-Krylov force, the diffraction force, and the radiation force (Patel, 1989). The Froude-Krylov force, realized as wave momentum, is imparted onto a submerged body, and the diffraction and radiation forces come from the disturbances to the surrounding fluid. The size of the buoy was considered significantly smaller than the length of the surface waves; as a result, the diffraction and radiation forces were considered negligible. Thus, the wave excitation force is equated to the Froude-Krylov force, as detailed below:

$$F_{excite} = -\rho_w \oiint \frac{\mathbf{d\Phi_i}}{dt}\widehat{n}\, dS_{submerged}. \tag{9}$$

In the above equation, the surface integral is taken over the submerged surface of the buoy. The normal vector to the surface is denoted by $\widehat{\mathbf{n}}$; since the simulation investigates one-dimensional motion, only the z-component of the normal vector is used.

Equations (4)–(9) can be combined together into equation (2) to create the governing equation of motion. It is impractical to solve analytically; instead numerical methods are used to calculate the position, velocity, and acceleration of the buoy at each time-step. The resulting data can be used to determine the RPM of the shaft, the tension in the cable, and the expected power output for a given generator model (C_{gen}).

In order to simulate the system as accurately as possible, it is necessary to analyze the system in three separate stages.

- **Stage I:** Decoupled stage (upper half of upstroke)—On the upper half of upstroke, the buoy deaccelerates. The sprocket decouples from the shaft, that is, the angular velocity of the shaft exceeds that of the sprocket; the pulling force of the buoy cable does not contribute work to the flywheel. Only the resistive force of the generator and friction exert forces on the shaft.
- **Stage II:** Down-stroke stage—On the down-stroke, there is no pulling force at the cable tethered in the buoy. The resistive load force of the generator is not applied as well, for the consideration of load control to keep flywheel momentum which forces the system to run continuously, although the frictional force (is proportional to angular velocity) slows the shaft.
- **Stage III:** Coupled stage (lower half of upstroke)—On the low half of

upstroke, the pulling force/torque accelerates the system until to the equilibrium point when the angular velocity of the shaft no longer increases. In addition to the pulling force, the resistive force of the generator and friction force also apply to the shaft, countering the pulling force/torque. The maximum tension is applied right after the lowest turning point.

Generator Model

The simulation of the system integrated the hydrodynamic force of the buoy into the mechanical and electrical models. For the experimental portion of this project, a GL-PMG-500A permanent magnet generator, manufactured by Ginlong Technologies, Inc., was utilized. This model has the advantage of a low start up torque (due to low cogging and resistive torque design) and high efficiency. The resistor load in this experiment is 1:6, which matches the resistive load tested by the generator's manufacturer. According to the generator specification, the power output can be represented as follows:

$$P = \frac{\left(\frac{w * 60}{2\pi}\right)^2}{16.6} \tag{10}$$

where w is the RPM of the shaft.

System Optimization

As mentioned previously, given a fixed wave amplitude and frequency, the optimal power output P_{max} depends on several factors. The radius of sprocket, r, the inertia of the flywheel(s), I, the ratio of the gear set used, GR, and the controlled electrical load added to the generator, L, may be adjusted to increase the power output of the system. The objective is to choose values for these parameters from their feasible ranges in an optimal way in order to get maximum power output. Of course the optimum values are dependent on the design of the buoy, and even more importantly, the wave conditions; the result is that in order to achieve truly optimum output, the parameters would have to dynamically adjust based on the constantly changing wave conditions. This is impractical, and instead the design parameters should be optimized based on the estimated average wave characteristics.

Matlab Simulation

A simulation was run in Matlab to determine the estimated power output using the one-dimensional scheme detailed in the previous section. In order to solve the differential equation given in equation (2), a fourth-order, explicit Runge-Kutta algorithm was implemented. The simulation is executed for a 60-s duration with a time-step of 0.05 s; initial conditions of dynamic equilibrium was imposed. The buoy is modeled simply as a sphere of radius R and the surface wave is a perfect sinusoid. Each design parameter may be adjusted independently within the simulation so as to determine the effect on the power output. The average power output is given for the 60-s simulation and used for comparison. Table 1 details the values of all of the constants used within the Matlab simulation.

The Matlab simulation is capable of outputting the instantaneous values of several system variables, including the tension in the mooring cable, the RPM of the shaft, and the generator output power. The simulation is run utilizing the inputs given in Table 1 (except for a 20-s duration).

The simulation is useful for predicting the average power output for given system inputs. Because the simulation uses arbitrary values for the parameters to be optimized, the results of this method are only suboptimal. To determine the actual optimal values, all parameters need to be varied simultaneously. For simplicity, only three design parameters are investigated here: flywheel inertia (I), the gear ratio (GR), and the load control threshold (L).

Flywheel Inertia Optimization

Without adequate inertia on the shaft, the flywheel may not continuously rotate throughout the complete wave cycle. With excessive inertia, on the other hand, the angular acceleration of the shaft will suffer as a result of increased chain tension, as seen in equations (6) and (2). As such, the inertia of the shaft should be optimized so that the motion of the shaft is continuous while limiting the effect on the buoy motion. Given a fixed wave amplitude and frequency, reasonable flywheel inertia can be chosen to maximize electrical power output. The value of the shaft inertia is varied in the Matlab simulation for values between 0.05 and 0.5 kg m^2; with increments of 0.01 kg m^2. The power output corresponding to the peak power is a function of the other parameters, but for the given inputs the optimal inertia for the shaft is found to be 0.25 kg m^2.

Gear Ratio Optimization

The generator detailed in the simulation is relatively small, with a low back-torque coefficient and ideal shaft

TABLE 1

Simulation parameter values for the optimization model.

Parameter	Value	Description
A_w	1	Amplitude of wave [m]
F	0.2	Frequency of wave [1/s]
R	0.5	Radius of buoy [m]
m	200	Mass of buoy [m]
ρ_w	997.0	Density of water at 25 °C [kg/m^3]
μ	0.001	Dynamic viscosity of water at 25 °C [kg/ms]
C_d	0.45	Drag coefficient of sphere [unit-less]
g	9.81	Gravitational acceleration [m/s^2]
T_o	100	Spool tension [kg m/s^2]
T_{fin}	60	Duration of model [s]
δt	0.02	Time step for model [s]
C_{gen}	6.36	Back-torque coefficient $\left[kg\,\frac{m^2}{s}\right]$
β_{fric}	0.5	Mechanical friction coefficient [kg m^2/s]
T_{start}	5	Start-up torque for generator [kg m/s^2]
I	0.1	Moment of Inertia of system [kg m^2]
GR	1.0	Gear ratio [unit-less]
L	0	Load control threshold [RPM]
R	0.05	Radius of sprocket [m]

input of around 275 RPM. To achieve this ideal speed, the gear ratio is likely to be on the order of, but greater than, unity. In the Matlab simulation, the gear ratio is a multiplier acting on the speed of the shaft and it acts to transmit the resulting large back-torques to the tension of the mooring line, as detailed in equation (6). The gear ratio is varied from 0.5 to 5, with increments of 0.1 in the simulation. Figure 4 illustrates the relationship between GR and the resulting average power output for the system.

FIGURE 4

Electrical power output vs. gear ratio.

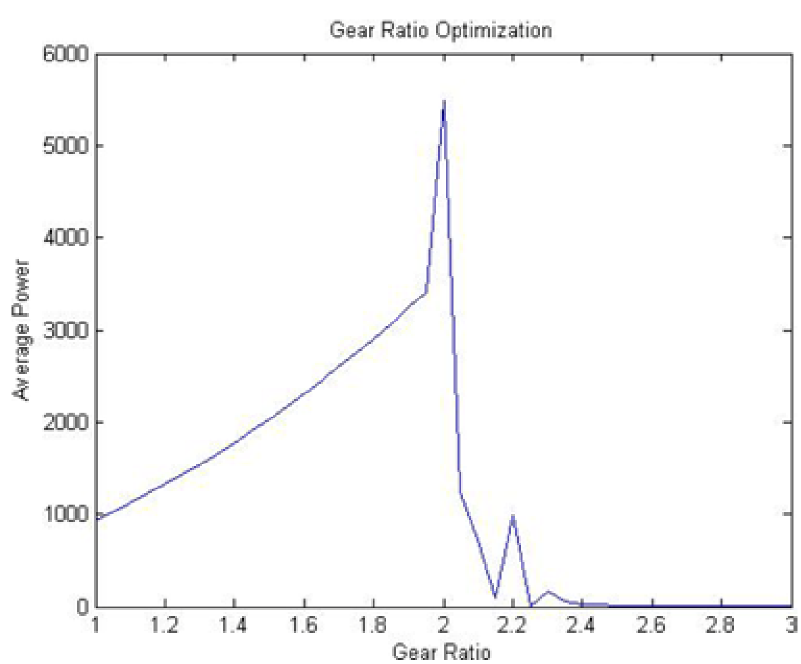

Electrical Load Control Optimization

By adjusting the timing at which the load is applied, continuous power extraction may be sacrificed in order to prevent the shaft from slowing to a standstill. Intuition suggests that the load should be applied while the shaft RPM is high above some threshold, and it should be disconnected while it becomes low. Furthermore, the electrical load should be controlled such that:

1. least load is applied in the down stroke when there is no wave force and
2. the oscillating velocity of the system is in phase with the wave's excitation force acting on the system (Kimoulakis & Kladas, 2008).

Usually the oscillating velocity of the buoy is out of phase with the wave's excitation force. Therefore, to maximize the electrical output power, the electrical load should be controlled in a way to make the buoy operate synchronously with the wave. The implementation of load control can be enhanced by selecting a threshold for which the load is disengaged. For example, if the RPM of the shaft drops below the threshold the load is reduced and then reengaged when the RPM rises above it. This load control threshold (LC) was a parameter in the Matlab simulation and varied from 0 to 200 RPM, at increments of 5 RPM.The suboptimal value for the load control threshold is found to be 170 RPM. Using this point as the threshold value, the electrical load is disconnected from the generator when the shaft speed falls below 170 RPM.

Optimization of the Sprocket Radius

The radius of the sprocket is directly related to the shaft RPM. The smaller the radius, the greater the RPM, but this also increases chain tension. The simulation did not demonstrate a clear relationship between sprocket size and power output; it appeared that the smaller the sprocket radius, the greater the power. It may be possible that a very small sprocket would provide an optimum size, but this would be impractical. Instead, the chosen sprocket is the smallest, commercially available unit that is sufficiently large enough to support the stresses induced by the peak chain tension.

Overall System Optimization

The suboptimal values found for the flywheel inertia, gear ratio, and the load control threshold are not very useful by themselves because of the arbitrary selection of values for the other parameters. To find the actual optimal values, all three parameters must be optimized simultaneously to account for system interdependencies. The three suboptimal values may serve as guidelines for where to inspect each of the parameters for the actual optimal values. For instance, when running the overall optimization simulation, values near 0.25 kg m^2 inertia, 2.0 gear ratio, and 170 RPM load threshold should be investigated as one or more may lie close to the actual system's optimum. The system scheme was done by brute force, a range around each of the aforementioned values was selected, and each scenario with that range was inspected to determine the highest power output. This method is effective, but highly inefficient. Nevertheless, optimum values were discovered for the given inputs for the defined buoy system and wave characteristics. The optimal parameters resulted in an inertia of 0.18 kg m^2, a gear ratio of 2.2, and load control of 190 (RPM).

Results and Discussion

Simulated Wave

In the laboratory prototype test, an electrical 6-DOF motion system is used to mimic the movement of ocean waves. The motion system consists of a motion platform, a base frame, a motion control cabinet, and a motion computer that can simulate the very complicated movements (i.e., a combination of lateral and vertical movements) of a buoy. Figure 1 is a simplified view of wave power generation system concept. All mechanical assemblies including the generator (shown at the upper right corner) are mounted to the motion platform. A chain is routed through a hole in the platform, and one end is attached to a pull-box directly tethered to the ground. The other end is fixed to the moving table. When the platform moves up, it pulls the chain to run over the sprockets to rotate the shaft; when the platform moves down, the pull-box tightens the chain.

Sensor Devices and Measurements

In the laboratory prototype testing, the following sensors are used to perform measurements to aide in optimizing the system. A strain gauge is used to measure the tension in the chain. This measurement is important in the design of the buoy to reduce the probability of a chain breaking due to excessive stress. An RPM encoder is used to measure the instantaneous RPM of the flywheel and generator. A displacement sensor is attached to the motion platform to measure the instantaneous height of the platform. This sensor is used in conjunction with a relay switch to automatically apply the electrical load at the most potent sections of the up-strokes.

Measurement of Voltage, Load Control, and RPM

The measurement of voltage, load control, and RPM under a frequency of 0.3 Hz and amplitudes (platform movement) of 10 cm and 12 cm were performed. After calculation, the average power output under the amplitude of 10 cm was 113.37 W. At an input amplitude of 12 cm, the system generated 136.13. Shaft RPMs were 188.60 and 221.42, respectively. This results in a 17.40% increase in RPM and a 20.08% increase in power (W) for experiments run with a flywheel with moment of inertia of 0.10 kg m^2.

A Comparison of Simulation and Experimental Results

Comparisons (RPM and power output) were made between the Matlab simulation and laboratory prototype results, at the same input torque; that is, the input torque based on the measured tension force in the prototype was used as the input torque to the Matlab simulation model.

Figure 5 shows the RPM data from both the simulation and the prototype unit. The experimental RPM is not smooth as the platform moves down; however, both datasets show similar patterns—RPMs increase quickly as the platform moves up and decrease slowly as the platform moves downward, a direct effect of the load control. When the RPM drops below the set threshold, the relay switch turns off, decreasing the electrical load. The momentum of the flywheels engages, and the shaft RPM decreases slowly as the energy stored in the flywheel momentum is depleted. Compared with the experimental results, the RPM in the simulation model drops more quickly at the beginning in the downstroke and then decays more slowly. It should be noted that the electrical load (its resistive torque) is much greater than the frictional torque in the mechanical system.

Several factors can cause the observed discrepancies. For example, it is difficult to measure the friction of the mechanical system or accurately simulate the generator model and its resistive torque. Furthermore, the motion platform can create a sinusoidal movement similar to a wave, but it is difficult to mimic the complex hydrodynamic buoy model, which includes several, more complex forces.

Conclusion

This paper introduces an innovative design, development, and laboratory prototype of a light-weight, low-cost, small-size wave power generation system which includes a buoy, a set of mechanical devices, and a permanent magnetic generator. Prior to prototype setup, a hydrodynamic model, buoy model, and a generator model were analyzed, and a Matlab system simulation was conducted. The flywheel inertia, shaft rotation speed, and electrical load are optimized to maximize electricity production. The current laboratory prototype is capable of generating an average of 136 W under the movement of a motion platform with 12 cm in amplitude, 0.3 Hz frequency, and 0.10 kg m^2 moment of inertia, and 206 W with 10 cm in amplitude, 0.3 Hz frequency, and 0.25 kg m^2 moment of inertia. System performance regarding the mechanical power input and electrical output was analyzed based on experimental data such as tension of the chain, shaft RPM, and voltage output. Both simulation and experimental results are provided and compared to verify the laboratory prototype design with reasonable correlation between them. The success of this mechanical system and optimized design could promise a clean, safe, and abundant energy source to satisfy a significant portion of society's energy needs in the future.

FIGURE 5

Comparison of RPM from Matlab simulation and prototype experimentation.

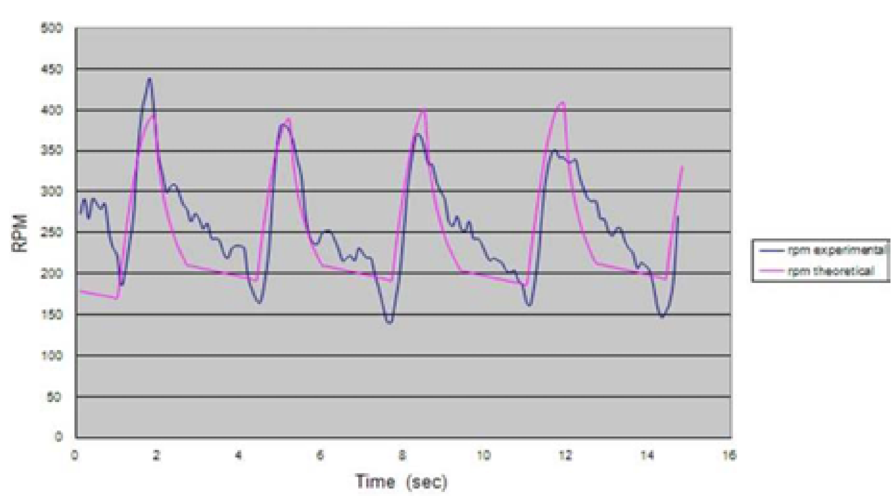

Corresponding Author:

Carlos Velez
Department of Mechanical and Aerospace Engineering,
University of Central Florida
4000 Central Florida Boulevard,
Orlando, FL 32826
Email: velezcar@yahoo.com

References

Brekken, T., von Jouanne, A., & Han, H. 2009. Ocean wave energy overview and research at Oregon State University. In: IEEE Power Electronics and Machines in Wind Applications, pp. 1-7. Lincoln, NE. Q1

Cunha, J., Lizarralde, F., Estefen, S., & Costa, P. 2009. Efficiency optimization in a wave energy hyperbaric converter. In: 2009 International Conference on Clean Electrical Power, vol. 20, pp. 68-75.

Elwood, D., Yim, S.C., von Jouanne, A., & Brekken, T. 2010. Experimental force characterization and numerical modeling of a taut-moored dual- body wave energy conversion system. J Offshore Mech Arct. 132:23-33. http://dx.doi.org/10.1115/1.3160535.

Eriksson, M., Isberg, J., & Leijon, M. 2005. Hydrodynamic modelling of a direct drive wave energy converter. Int J Eng Sci. Q2

43:1377-87. http://dx.doi.org/10.1016/j.ijengsci.2005.05.014.

Q3 **Falnes**, J. 2002. Ocean Waves and Oscillating Systems. Cambridge University Press. 12 pp. http://dx.doi.org/10.1017/CBO9780511754630.

Haniotis, A., Papathanassiou, S., Kladas, A., & Papadopoulos, M. 2002. Control issues of a permanent-magnet generator, variable-speed, wind turbine. Wind Eng. 26:371-81. http://dx.doi.org/10.1260/030952402765173367.

Kimoulakis, N., & Kladas, A. 2008. Modeling and control of a coupled electromechanical system exploiting heave motion, for energy conversion from sea waves. In: IEEE Power Electronics Specialists Conference, pp. 3850-3. Rhodes, Greece: IEEE. http://dx.doi.org/10.1109/TMAG.2007.914854.

Kimoulakis, N., Kladas, A., & Tegopoulos, J. 2008. Power generation optimization from sea waves by using a permanent magnet linear generator drive. IEEE T Magn. 44(6):1530-3.

Leijon, M., Bernhoff, H., Agren, O., Isberg, J., Sundberg, J., Berg, M., … Wolfbrandt, A. 2005. Multiphysics simulation of wave energy to electric energy conversion by permanent magnet linear generator. IEEE T Energy Conver. 20:219-24. http://dx.doi.org/10.1109/TEC.2004.827709.

Q4 **Leonard**, J.W., Idris, K., & Yim, S. 2000. Large angular motions of tethered surface buoys. Ocean Eng. 27:1345-71. http://dx.doi.org/10.1016/S0029-8018(99)00046-3.

Mueller, M., & Baker, N. April 2002. A low speed reciprocating permanent magnet generator for direct drive wave energy converter. In IEEE Conference on Power Electronics, Machines and Drives, pp. 468-73. Bath, UK: IEEE. http://dx.doi.org/10.1049/cp:20020162.

Q5 **Osawa**, H., Washio, Y., Ogata, T., & Tsuritani, Y. 2002. The offshore floating type wave power device mighty whale open sea tests. In Proceedings of the 12th International Offshore and Polar Engineering Conference, pp. 595-600. Kitakyushu, Japan.

Patel, M. 1989. Dynamics of Offshore Structures. UK: VButterworth-Heinemann. 45 pp.

Rhinefrank, K., Agamloh, E., von Jouanne, A., Wallace, A., & Prudell, J. 2006. Novel ocean energy permanent magnet linear generator buoy. Renew Energ. 31:1279-98. http://dx.doi.org/10.1016/j.renene.2005.07.005.

Sarpkaya, T., & Isaacson, M. 1981. Mechanics Q6 of Wave Forces on Offshore Structures. Van Nostrand Reinhold Company. 36 pp.

Wolfbrandt, A. 2006. Automated design of a linear generator for wave energy converters: A simplified model. IEEE T Magn. 42:1812-9. http://dx.doi.org/10.1109/TMAG.2006.874593.